


Dynamic contrast-enhanced MR imaging pharmacokinetic parameters as predictors of treatment response of brain metastases in patients with lung cancer

Grégory Kuchcinski¹  · Emilie Le Rhun^{2,3,4} · Alexis B. Cortot⁵ · Elodie Drumez⁶ · Romain Duhal¹ · Maxime Lalisse¹ · Julien Dumont¹ · Renaud Lopes¹ · Jean-Pierre Pruvo¹ · Xavier Leclerc¹ · Christine Delmaire¹

Received: 28 October 2016 / Revised: 4 January 2017 / Accepted: 19 January 2017 / Published online: 16 February 2017
© European Society of Radiology 2017

Abstract

Objectives To determine the diagnostic accuracy of pharmacokinetic parameters measured by dynamic contrast-enhanced (DCE) magnetic resonance imaging (MRI) in predicting the response of brain metastases to antineoplastic therapy in patients with lung cancer.

Methods Forty-four consecutive patients with lung cancer, harbouring 123 newly diagnosed brain metastases prospectively underwent conventional 3-T MRI at baseline (within 1 month before treatment), during the early (7–10 weeks) and midterm (5–7 months) post-treatment period. An additional DCE MRI sequence was performed during baseline and early post-treatment MRI to evaluate baseline pharmacokinetic parameters (K^{trans} , k_{ep} , v_e , v_p) and their early variation

(ΔK^{trans} , Δk_{ep} , Δv_e , Δv_p). The objective response was judged by the volume variation of each metastasis from baseline to midterm MRI. ROC curve analysis determined the best DCE MRI parameter to predict the objective response.

Results Baseline DCE MRI parameters were not associated with the objective response. Early ΔK^{trans} , Δv_e and Δv_p were significantly associated with the objective response ($p = 0.02$, $p = 0.001$ and $p = 0.02$, respectively). The best predictor of objective response was Δv_e with an area under the curve of 0.93 [95% CI = 0.87, 0.99].

Conclusions DCE MRI and early Δv_e may be a useful tool to predict the objective response of brain metastases in patients with lung cancer.

Key Points

- DCE MRI could predict the response of brain metastases from lung cancer
- Δv_e was the best predictor of response
- DCE MRI could be used to individualize patients' follow-up

Electronic supplementary material The online version of this article (doi:10.1007/s00330-017-4756-5) contains supplementary material, which is available to authorized users.

✉ Grégory Kuchcinski
gregory.kuchcinski@univ-lille2.fr

Keywords Magnetic resonance imaging · Perfusion · Blood-brain barrier · Brain neoplasms · Lung neoplasms

¹ Department of Neuroradiology, University of Lille, CHU Lille, Rue Emile Laine, F-59000 Lille, France

² Department of Neurosurgery, University of Lille, CHU Lille, F-59000 Lille, France

³ Department of Medical Oncology, Oscar Lambret Center, F-59000 Lille, France

⁴ Inserm U1192-PRISM-Laboratoire de Protéomique, Réponse Inflammatoire, Spectrométrie de Masse, F-59000 Lille, France

⁵ Department of Thoracic Oncology, University of Lille, CHU Lille, F-59000 Lille, France

⁶ Department of Biostatistics, University of Lille, CHU Lille, EA 2694-Santé publique: épidémiologie et qualité des soins, F-59000 Lille, France

Abbreviations

AUC	Area under the curve
BBB	Blood-brain barrier
CI	Confidence interval
DCE	Dynamic contrast-enhanced
EGF-R	Epidermal growth factor receptor
FLAIR	Fluid-attenuated inversion recovery
ICC	Intraclass correlation coefficient
IQR	Interquartile range
k_{ep}	Rate constant
K^{trans}	Transfer constant

KPS	Karnofsky performance status
MRI	Magnetic resonance imaging
OR	Odds ratio
OS	Overall survival
PFS	Progression-free survival
ROC	Receiver-operating characteristics
v_e	Extravascular extracellular space per unit volume of tissue
v_p	Plasmatic space per unit volume of tissue

Introduction

Lung cancer is the most frequent cancer worldwide and the most common cause of cancer death [1]. Brain metastases occur in 10–20% of patients with localized lung cancer [2] and severely impact the quality of life and the overall survival (OS) [3]. The therapeutic strategy for brain metastasis is mainly based on local treatments such as surgery, radiosurgery or whole-brain radiotherapy [4] and depends on the number, localization and size of brain metastases, control of extra-central nervous system disease and the general condition of patients. Systemic therapy alone may be considered in asymptomatic patients [5].

Current guidelines for brain metastases assessment are based on size variation on conventional magnetic resonance imaging (MRI), but radiological enlargement during the early post-treatment period does not necessarily represent tumour progression, especially in patients treated by radiosurgery or targeted therapy [6]. Given the potential benefits of second-line therapies [5], it is crucial to determine predictors of response during the early follow-up. Previous studies have demonstrated the increasing abilities of advanced MRI techniques to predict the response in patients with brain metastases, including the apparent diffusion coefficient of diffusion-weighted imaging [7], the relative cerebral blood volume using dynamic susceptibility-contrast MRI perfusion [8] and the metabolic changes using MR spectroscopy [9]. However, the relevance of these techniques remains widely debated for patient management in routine clinical practice.

Dynamic contrast-enhanced (DCE) MRI is a minimally invasive method (requiring intravenous injection of gadolinium) which enables the assessment of the blood-brain barrier (BBB) integrity and neoangiogenesis within brain tumours [10]. When a two-compartment model is used [11], DCE MRI provides different pharmacokinetic parameters: (i) the volume transfer constant (K^{trans}), reflecting the BBB permeability; (ii) the extravascular extracellular space per unit volume of tissue (v_e); (iii) the plasmatic space per unit volume of tissue (v_p); (iv) the rate constant (k_{ep}), which is a K^{trans}/v_e ratio.

The diagnostic and prognostic value of DCE MRI has been well demonstrated in gliomas [12, 13] and extracranial neoplasms [14, 15] but it has been scarcely evaluated in the post-

treatment assessment of brain metastases despite promising results [16, 17].

We hypothesized that increased BBB permeability and neoangiogenesis in brain metastases were associated with a better response to antineoplastic therapy and that the early variation of the DCE MRI parameters was predictive of the objective response.

The purpose of our study was to determine the diagnostic accuracy of pharmacokinetic parameters measured by DCE MRI to predict the response of brain metastases to antineoplastic therapy in patients with lung cancer.

Materials and methods

Patients

This was a monocentric prospective observational longitudinal diagnostic study without randomization (NCT02250755), approved by the institutional review board (no. 2012-A011164-39). Written informed consent was obtained from all patients.

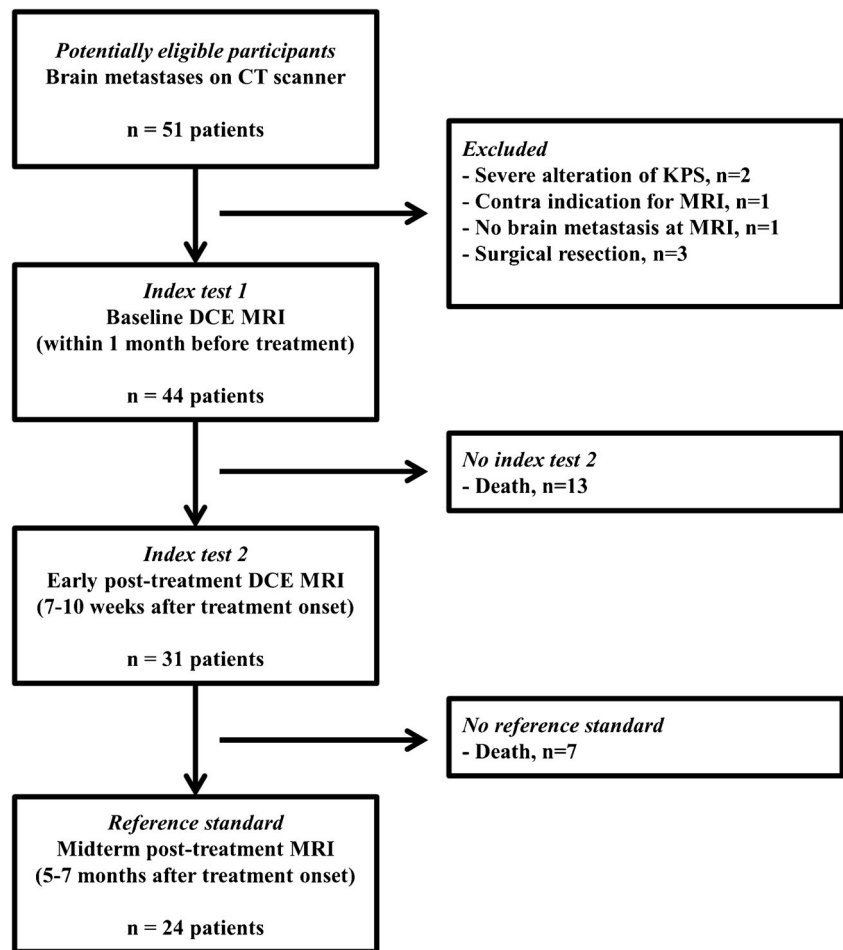
We prospectively screened all adult patients with histologically proven lung cancer, and newly diagnosed brain metastases on systematic computed tomography scan treated at our institution between April 2012 and December 2014. Exclusion criteria were (a) neurosurgical treatment of brain metastases; (b) prior brain metastases; (c) Karnofsky performance status (KPS) <60; (d) contraindication to MRI and (e) inability to consent. As a result, 44 patients were included (33 men, 11 women) (Fig. 1).

Pathological analysis of primary lung cancer, age, KPS, presence of extracranial metastases and oncologic treatment (systemic therapy, whole-brain radiotherapy, radiosurgery) were prospectively recorded at the diagnosis and during a follow-up period of 6 months following the treatment onset. Treatment strategy was decided by multidisciplinary agreement according to current guidelines [4].

MRI protocol

MRI studies were performed at baseline (within 1 month before treatment), early (7–10 weeks) post-treatment period and mid-term (5–7 months) post-treatment period on a 3-T MRI scanner (Philips Achieva, Philips Medical Systems, Best, the Netherlands). Conventional sequences, including a post-contrast 3D gradient-echo T1-weighted sequence, were performed in all MRI examinations (Supplemental Table 1). A DCE MR sequence was added to baseline and early MRI. The dynamic acquisition (TR/TE = 14/3 ms, flip angle = 15°, voxel = 1.25 × 1.25 × 3 mm, 22 axial sections, 65 dynamics, temporal resolution = 6 s, duration = 6 min 46 s) was performed after two fast-gradient echo T1-weighted sequences with

Fig. 1 Flow chart of the study. *CT* computed tomography, *DCE* dynamic contrast-enhanced, *KPS* Karnofsky performance status, *MRI* magnetic resonance imaging



different flip angles ($\alpha = 5^\circ$ and 20°). Gadolinium (gadoteric acid, DOTAREM®, 0.1 mmol/kg, relaxivity = $3.3 \text{ mM}^{-1} \text{ s}^{-1}$ at 3 T, injection rate 5–7 mL/s) was administrated intravenously 48 s after the beginning of the acquisition.

DCE MRI analysis

DCE MRI analysis was performed by a neuroradiologist (15 years of experience) blinded to clinical and volumetric data, using the PRIDE software (Philips). K^{trans} , k_{ep} , v_e and v_p maps were generated automatically according to the bicompartamental modified Tofts model [11]. Preprocessing steps consisted of rigid realignment for motion correction and exclusion of the voxels located outside the skull. A T1 mapping was computed from three fast-gradient echo T1-weighted acquisitions with different flip angles ($\alpha = 5^\circ$, 15° , 20°). An individual arterial input function was determined: several regions of interest (ROI) were manually placed in the internal carotid arteries, middle cerebral arteries and superior sagittal sinus to obtain the best enhancement curve. For DCE MRI measurements, mean K^{trans} , k_{ep} , v_e and v_p were

measured in an ROI manually placed on the enhancing part of each lesion on the dynamic acquisition, at the level of the maximum section area to minimize partial volume effect, and copied to the K^{trans} , k_{ep} , v_e and v_p maps (Fig. 2). Necrotic and cystic areas were carefully excluded. The minimum area of the ROI was 20 mm^2 . At early follow-up, ΔK^{trans} , Δk_{ep} , Δv_e and Δv_p were calculated according to the following formula: $\Delta K^{\text{trans}} = (\text{early } K^{\text{trans}} - \text{baseline } K^{\text{trans}}) / \text{baseline } K^{\text{trans}}$. Changes in DCE MRI parameters had no impact on the subsequent treatment strategy.

To assess the reliability of the method, mean K^{trans} , k_{ep} , v_e and v_p were blindly measured on baseline MRI by two independent observers (with 6 and 15 years of experience).

Volumetric analysis A neuroradiologist (25 years of experience), blinded to DCE MRI and clinical data, measured the volume of each metastasis, using a semi-automated segmentation method, on the post-contrast 3D T1-weighted sequence. The midterm response, determined according to the volume variation of each brain metastasis from baseline to midterm using a volumetric adaptation of the RECIST 1.1 criteria, was

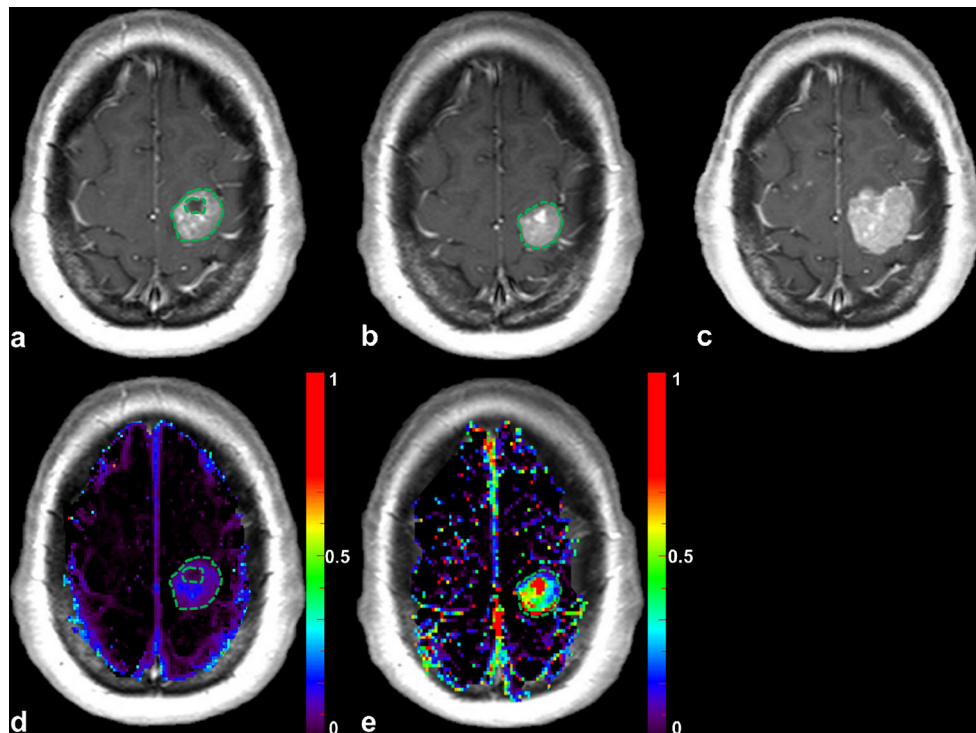


Fig. 2 Illustrative case. Patient with a left precentral metastasis on T1-weighted images at baseline (a), early follow-up (b) and midterm follow-up (c) and parametric map of v_e at baseline (d) and midterm follow-up (e). A volumetric regression of the lesion was observed on the conventional T1-weighted sequence with gadolinium injection between baseline (a) and early follow-up (b). On the contrary, DCE MRI parametric map demonstrated an increase of the v_e value between baseline (d) and early

follow-up (e), which predicted the volumetric progression of the lesion at midterm follow-up (c). The *green dotted line* represents the region of interest used for DCE MRI measurement at baseline (a, d) and early follow-up (b, e), corresponding to the enhancing part of the lesion at the level of maximum section area with careful exclusion of necrotic components

considered as the reference standard: a decrease of 65% or more was considered a positive response, an increase of more than 73% was considered as progression and a variation between -65% and $+73\%$ was considered as stable disease [18].

Statistical analysis

The interobserver reliability was calculated with Fleiss intraclass correlation coefficient (ICC) using a two-way mixed model and interpreted as follows: poor agreement, <0.45 ; fair to good agreement, between 0.45 and 0.75; and excellent agreement, >0.75 [19].

The primary endpoint was the diagnostic accuracy of DCE MRI parameters in predicting the midterm response, in the terms of metastases assessment. The association between DCE MRI parameters and the midterm response was explored using mixed logistic regression models to take into account the within-subject correlation (DCE MRI parameters as fixed effects, patients as random effect). Receiver-operating characteristics (ROC) curves were computed using the predicted probabilities from the fitted mixed logistic model to estimate the area under the curve (AUC). Optimal thresholds were calculated by maximizing the sensitivity and specificity using the fixed effects. We compared the diagnostic accuracy of

conventional MRI with and without the addition of the best parameter using a logistic model. The correlation between ΔK^{trans} , Δk_{ep} , Δv_e , Δv_p and the volumetric variation of each brain metastasis at midterm follow-up was analysed using a Spearman's rank correlation coefficient (r).

In terms of patient response, OS and progression-free survival (PFS) at 6 months were determined using the Kaplan–Meier method. We studied the association between clinical prognostic factors (age < 60 years, KPS ≥ 90 , number of brain metastasis [solitary versus more than one], presence of extracranial metastases) [20] and OS or PFS using log-rank tests. The association between baseline DCE MRI parameters and OS or PFS was explored using univariate Cox's regression. Hazard ratio and its 95% confidence interval (CI) were derived from Cox's regression models as effect size measures. We assessed the log-linearity assumption for each parameter using Martingale residual plots and the proportional hazards assumption by plotting the Schoenfeld residuals against the rank of survival time [21]. For patients with multiple brain metastases, K^{trans} , k_{ep} , v_e and v_p were defined as the maximum value among the patient's metastases.

Data were analysed using the SAS software, release 9.4 (SAS Institute, Cary, NC). A p value less than 0.05 indicated a statistically significant difference.

Results

Population

Baseline characteristics of the 44 patients (with 123 brain metastases) are presented in Tables 1 and 2. Median age was 58 years. The most frequent histopathology was adenocarcinoma (68.2% of the patients), followed by small cell carcinoma (25% of the patients). Brain metastases were diagnosed after a median time of 9.1 months [interquartile range (IQR) = 3–14.2] from lung cancer diagnosis. At the time of brain metastases diagnosis, 36 (81.8%) patients had concurrent extracranial metastases. Brain metastases were symptomatic in 6

Table 1 Clinical, histopathological and radiological characteristics of the patients at baseline ($n = 44$ patients)

Characteristics	Value
Clinical characteristics	
Age, years, median [IQR]	58 [55–64]
Male sex, n (%)	33 (75)
KPS, median [IQR]	90 [80–90]
Neurologic symptoms, n (%)	6 (13.6)
Histopathology of primary cancer	
Non-small cell carcinoma, n (%)	33 (75)
Adenocarcinoma	30 (68.2)
With EGF-R mutation	4 (9.1)
Squamous cell carcinoma	2 (4.6)
Indeterminate	1 (2.3)
Small cell lung carcinoma, n (%)	11 (25)
Number of previous chemotherapy lines, median [IQR]	1 [0–2]
Current systemic therapy, n (%)	16 (36.4)
Platinum-based chemotherapy	6 (13.6)
Antiangiogenic therapy	1 (2.3)
Other targeted therapy	3 (6.8)
Other	6 (13.6)
Local staging (T)	
Tx	3 (6.8)
T1	5 (11.4)
T2	15 (34.1)
T3	7 (15.9)
T4	14 (31.8)
Regional staging (N)	
N0	4 (9.1)
N1	3 (6.8)
N2	17 (38.6)
N3	20 (45.5)
Extracranial metastases	
Lung metastases	10 (22.7)
Other	26 (59.1)

EGF-R epidermal growth factor receptor, IQR interquartile range, KPS Karnofsky performance status

(13.6%) patients. The median KPS was 90. Solitary brain metastases were found in 17 (38.6%) patients, 2 or 3 brain metastases in 14 (31.8%) and more than 3 brain metastases in 11 (25%). Median pretreatment volume of the brain metastases was 400 mm³ [IQR = 110–1240]. At baseline, median K^{trans} , k_{ep} , v_e and v_p were 0.04 min⁻¹ [IQR = 0.02–0.06], 0.23 min⁻¹ [IQR = 0.16–0.31], 0.18 [IQR = 0.13–0.25] and 0.04 [IQR = 0.03–0.05], respectively. The measurement reliability evaluated by ICC demonstrated an excellent agreement for K^{trans} , k_{ep} , v_e and v_p (Table 3).

Follow-up

Median time from baseline MRI to treatment onset was 19 days [IQR = 7–27]. The early MRI was performed at a median time of 8 weeks [IQR = 7–10] after the treatment onset and the midterm MRI at a median time of 6 months [IQR = 5–7]. One patient had a modification of treatment between early and midterm follow-up, consisting of a modification of the systemic therapy regimen.

Clinical outcome

Twenty four patients were alive at midterm follow-up, with an OS rate of 54.5% [95% CI = 38.8, 67.8]; of these, 18 had stable disease or better, giving a PFS rate of 40.9% [95% CI = 26.5, 54.8] (Fig. 3). Causes of death were neurological in 5 (25%) patients, extracranial in 11 (55%) [thoracic progression in 6, pneumonia in 3, liver failure in 1, renal failure in 1] and unknown in 4 (20%). OS at midterm follow-up was significantly better in patients less than 60 years of age ($p = 0.04$) and with KPS ≥ 90 ($p = 0.002$) (Fig. 4). There was a trend towards worse OS with multiple brain metastases ($p = 0.08$) and the presence of extracranial metastasis ($p = 0.06$); however, this was not statistically significant. Similar results were observed for PFS (data not shown). Conversely, baseline DCE MRI parameters were not significantly associated with the OS or PFS (Table 4).

Radiological outcome

Regarding to volumetric analyses at midterm follow-up, the objective response was evaluated for 61 brain metastases in 24 surviving patients. Positive response on MRI was observed in 46 brain metastases and non-response in the 15 remaining metastases (progression in 7 and stable disease in 8). When the volumetric adaptation of the RECIST 1.1 criteria was used, conventional MRI at early follow-up had a sensitivity of 0.76 [95% CI = 0.61, 0.87] and a specificity of 0.73 [95% CI = 0.51, 0.95] in predicting a positive response at midterm follow-up.

Regarding DCE MRI analyses, the baseline values of DCE MRI pharmacokinetic parameters and their early variation,

Table 2 Treatment strategy ($n = 44$ patients)

Antineoplastic therapy	n (%)
Radiosurgery	10 (22.7)
Without adjuvant systemic therapy	5 (11.4)
With adjuvant systemic therapy	5 (11.4)
Platinum-based chemotherapy	3 (6.8)
Antiangiogenic therapy	2 (4.5)
Other targeted therapy	0 (0)
Other	1 (2.3)
Whole-brain radiotherapy	11 (25)
Without adjuvant systemic therapy	4 (9.1)
With adjuvant systemic therapy	7 (15.9)
Platinum-based chemotherapy	2 (4.5)
Antiangiogenic therapy	1 (2.3)
Other targeted therapy	2 (4.5)
Other	3 (6.8)
Systemic therapy alone	23 (43.2)
Platinum-based chemotherapy	10 (22.7)
Antiangiogenic therapy	4 (9.1)
Other targeted therapy	4 (9.1)
Other	9 (20.5)

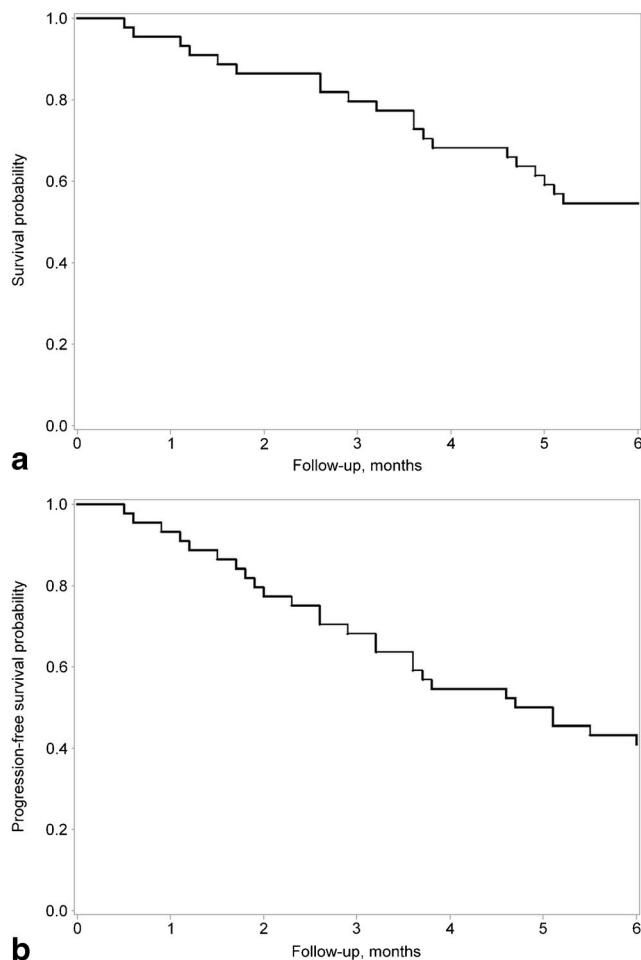
according to the objective response at midterm follow-up, are presented in Table 5. Baseline K^{trans} , k_{ep} , v_e and v_p were not associated with the objective response at midterm follow-up (Table 6). However, early ΔK^{trans} , Δv_e and Δv_p were significantly associated with the objective response at midterm follow-up ($p = 0.02$, $p = 0.001$ and $p = 0.02$, respectively) (Table 6). The best parameter to predict a positive response was Δv_e with an AUC of 0.93 [95% CI = 0.87, 0.99] (Figs. 2 and 5). The optimal threshold for Δv_e was $< -12.5\%$ with a sensitivity of 0.87 [95% CI = 0.74, 0.95] and a specificity of 0.80 [95% CI = 0.52, 0.96]. The addition of Δv_e to conventional MRI in the prediction model significantly improved the diagnostic accuracy: AUC = 0.82 [95% CI = 0.70, 0.95] for

Table 3 ICC for the DCE MRI pharmacokinetic parameters measured by two observers ($n = 123$ metastases)

	ICC	95% CI
K^{trans}	0.785	[0.699, 0.853]
k_{ep}	0.929	[0.899, 0.951]
v_e	0.848	[0.748, 0.911]
v_p	0.837	[0.646, 0.913]

ICC values were interpreted as follows: poor agreement for values, < 0.45 ; fair to good agreement for values, between 0.45 and 0.75; and excellent agreement for values, > 0.75

CI confidence interval, DCE dynamic contrast-enhanced, ICC intraclass correlation coefficient, MRI magnetic resonance imaging

**Fig. 3** Kaplan–Meier overall (a) and progression-free (b) survival curves of the 44 patients at midterm follow-up. Death occurred in 20 patients during the follow-up, progression in 26 patients

conventional MRI vs AUC = 0.94 [95% CI = 0.88, 1.00] for conventional MRI + Δv_e , $p = 0.03$ (Fig. 6).

In each treatment subgroup, we found a strong correlation between early Δv_e and the volumetric variation of each brain metastasis at midterm follow-up (radiosurgery, $r = 0.843$, $p = 0.002$; radiotherapy, $r = 0.589$, $p < 0.001$; systemic therapy, $r = 0.813$, $p < 0.001$).

In the subgroup of patients with multiple brain metastases, the risk of global non-response at midterm follow-up was higher for patients having at least one metastasis with $\Delta v_e > -12.5\%$ (3/6) in comparison with patients without metastasis with $\Delta v_e > -12.5\%$ (1/5).

Discussion

In this study conducted in patients with brain metastases from lung cancer, treated either by radiosurgery, whole-brain radiotherapy or systemic therapy alone, we found that the early variation of v_e (7–10 weeks post-treatment) was the best

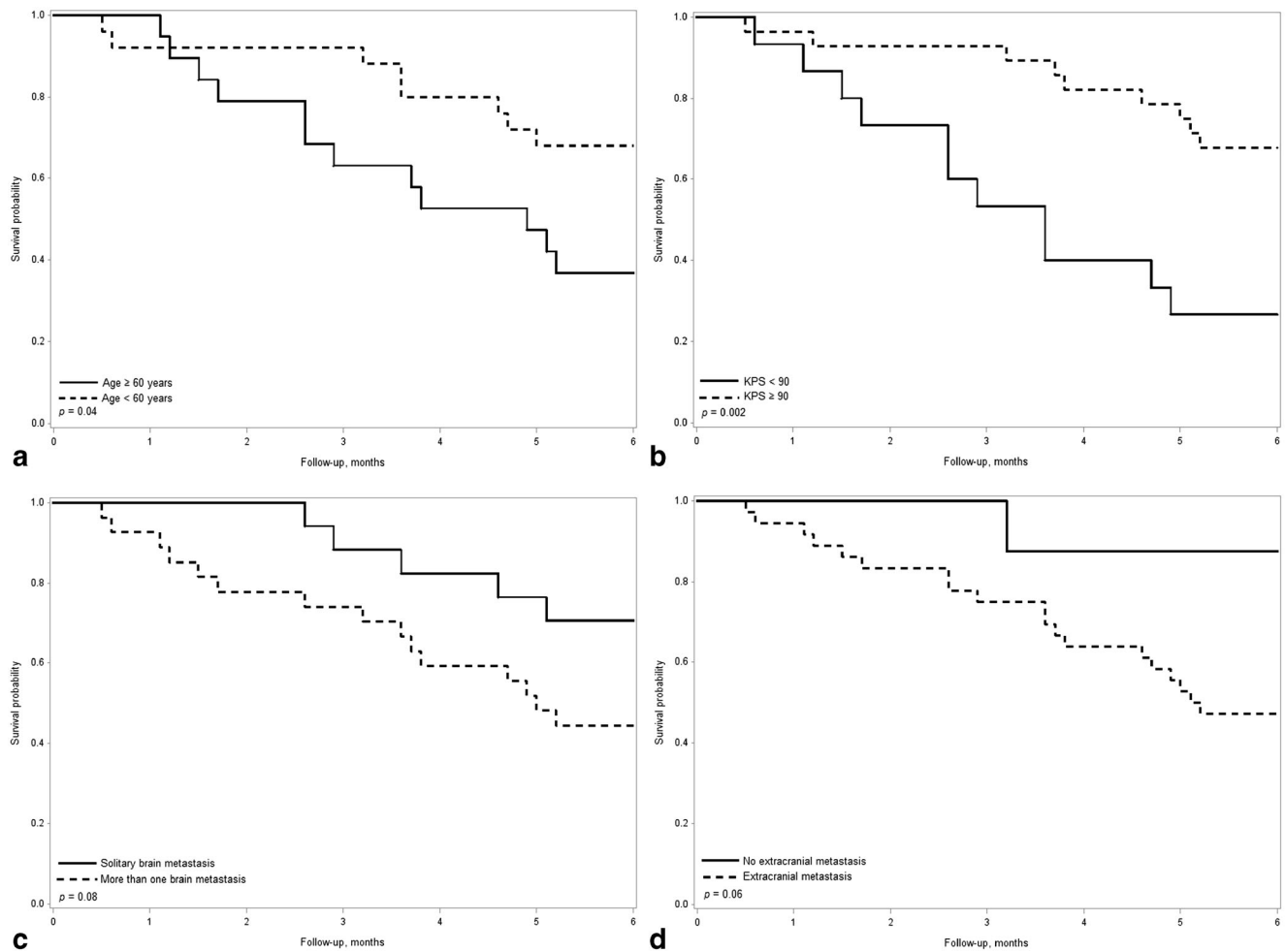


Fig. 4 Kaplan–Meier survival curves of the 44 patients for 4 clinical prognostic factors demonstrated a better survival in patients < 60 years (a), with KPS \geq 90 (b), with a solitary brain metastasis (c) and without extracranial metastasis (d)

predictor of response at midterm follow-up. We also found a moderate but significant association between ΔK^{trans} and the objective response.

To our knowledge, the prognostic value of the early variation of v_e in brain metastases has not been previously reported. In brain neoplasms, neoangiogenesis generates leaky vessels,

with altered endothelial tight junctions, leading to plasma extravasation into the extravascular extracellular space [22]. DCE MRI enables a quantitative assessment of the extravascular extracellular space expansion within each voxel through the pharmacokinetic parameter v_e , which is elevated in brain metastases [23], glioblastomas and various extracranial tumours [24, 25]. The antiangiogenic effect of radiotherapy and systemic therapy is responsible for a reduction of vascular permeability and plasma extravasation in brain tumours. Accordingly, glioblastomas treated by antiangiogenic therapies [26, 27] and/or radiotherapy [28] exhibit a 20–30% post-treatment reduction of v_e . Histopathological studies in mice confirmed decreased water content in glioblastomas treated by antiangiogenic therapy and demonstrated that it was associated with better survival [29].

In two previous studies evaluating DCE MRI in the assessment of brain metastases after radiotherapy, v_e was not evaluated but the variation of K^{trans} was reported as a good predictor of response. Jakubovic et al. [16], in 44 patients with 70 brain metastases treated by radiosurgery, found a lower K^{trans} at

Table 4 Risk of death and progression at midterm follow-up by pre-treatment values of pharmacokinetic parameters (n = 44 patients)

Variables	Risk of death		Risk of progression	
	HR [95% CI]	p	HR [95% CI]	p
K^{trans}	1.08 [0.96, 1.22]	0.20	1.04 [0.93, 1.16]	0.46
k_{ep}	1.00 [0.96, 1.04]	0.87	0.98 [0.95, 1.02]	0.39
v_e	1.00 [0.98, 1.02]	0.89	1.00 [0.98, 1.02]	0.69
v_p	1.01 [0.92, 1.12]	0.82	0.99 [0.91, 1.09]	0.89

Hazard ratio calculated per 0.01-unit increase

HR hazard ratio

Table 5 Baseline values of DCE MRI pharmacokinetic parameters and their variation at early follow-up according to the objective response at midterm follow-up ($n = 61$ metastases)

	Baseline DCE MRI					Variation between baseline and early follow-up			
	Midterm response ($n = 46$)		Midterm non-response ($n = 15$)			Midterm response ($n = 46$)		Midterm non-response ($n = 15$)	
	Median	IQR	Median	IQR		Median	IQR	Median	IQR
K^{trans} (min^{-1})	0.04	[0.02, 0.06]	0.04	[0.02, 0.05]	ΔK^{trans}	-50%	[-100, 0]	-20%	[-38, +33]
k_{ep} (min^{-1})	0.22	[0.13, 0.36]	0.19	[0.14, 0.30]	Δk_{ep}	-20%	[-60, +40]	-15%	[-58, +22]
v_e	0.18	[0.13, 0.24]	0.18	[0.11, 0.29]	Δv_e	-71%	[-97, -27]	+31%	[-10, +127]
v_p	0.04	[0.03, 0.05]	0.04	[0.04, 0.05]	Δv_p	-63%	[-80, -33]	-20%	[-25, 0]

DCE dynamic contrast-enhanced, IQR interquartile range, MRI magnetic resonance imaging

1 week in responding lesions. Similarly, Almeida-Freitas et al. reported an increase of K^{trans} 4–8 weeks after radiosurgery associated with midterm progression in 26 patients with 34 brain metastases [17]. In the present study, we found a moderate association between ΔK^{trans} and the objective response. Post-treatment vascular changes are highly time dependent and the timing of early MRI evaluation may account for this partial discrepancy. In the study of Jakubovic et al., K^{trans} was significantly associated with tumour response when measured at 1 week after treatment, but the association was no longer significant at 1 month [16]. In our study, the early MRI evaluation was performed 7–10 weeks after treatment, which is in agreement with the routine follow-up of patients with brain metastases and therefore practical in a clinical setting. Nevertheless, the optimal timing of the early MRI evaluation remains to be determined.

As reported in earlier studies [16, 17], we did not find any association between pretreatment DCE MRI parameters and the objective response. BBB is considered to be the main limitation to the efficacy of chemotherapy on brain metastases [30, 31] and is the target of many research projects such as selective alteration of the BBB [32, 33] and development of drugs going through the BBB [34]. However, conversely to preclinical reports in animal models [35], baseline BBB permeability evaluated by K^{trans} did

not significantly differ between responding and non-responding lesions in the present study.

We showed that a cut-off value of $\Delta v_e > -12.5\%$ predicted the midterm response with an improved diagnostic accuracy in comparison to conventional MRI. According to current guidelines, conventional MRI with gadolinium injection is the standard reference for brain metastases assessment [6]. However, transient volume variations may occur in the early follow-up after radiotherapy [36] or targeted therapy [37] and are not predictive for long-term outcome. Thus, despite an increased scan time, an additional DCE MRI sequence allows a more comprehensive analysis of neoangiogenesis modifications. On the basis of our results and given the potential benefits of second-line treatments, metastases with a stable or increased v_e (i.e. $\Delta v_e > -12.5\%$) during the early post-treatment period would benefit from short-interval MRI follow-up to anticipate the diagnosis of tumour progression. In case of multiple brain metastases and heterogeneous response, the added value of DCE MRI remains undetermined but our preliminary results suggest that the risk of global non-response is higher in patients with at least one metastasis with $\Delta v_e > -12.5\%$.

Our study had several limitations. First, the limited size of our cohort precluded accurate evaluation of DCE MRI in each

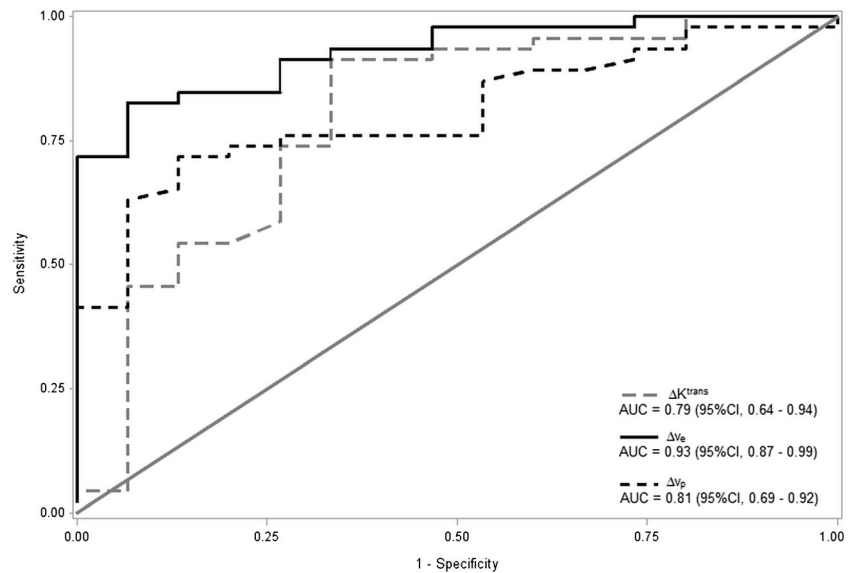
Table 6 Association between DCE MRI pharmacokinetic parameters and positive response at midterm follow-up ($n = 61$ metastases)

	Baseline DCE MRI				Variation between baseline and early follow-up		
	OR	95% CI	p		OR	95% CI	p
K^{trans}	2.88	[0.23, 36.7]	0.41	ΔK^{trans}	0.87	[0.78, 0.97]	0.02
k_{ep}	1.32	[0.75, 2.32]	0.33	Δk_{ep}	1.02	[0.94, 1.11]	0.65
v_e	1.20	[0.70, 2.07]	0.50	Δv_e	0.77	[0.66, 0.90]	0.001
v_p	2.30	[0.23, 23.3]	0.47	Δv_p	0.82	[0.70, 0.97]	0.02

OR calculated per 0.01-unit increase for baseline parameters and OR per 10-unit increase for parameters variations

CI confidence interval, DCE dynamic contrast-enhanced, OR odds ratio, MRI magnetic resonance imaging

Fig. 5 ROC curves analysis for DCE MRI parameters. Δv_e provided the best predictive value for a positive response at midterm follow-up with an area under the receiver operating curve of 0.93 [95% CI = 0.87, 0.99]. *AUC* area under the receiver operating characteristics curve



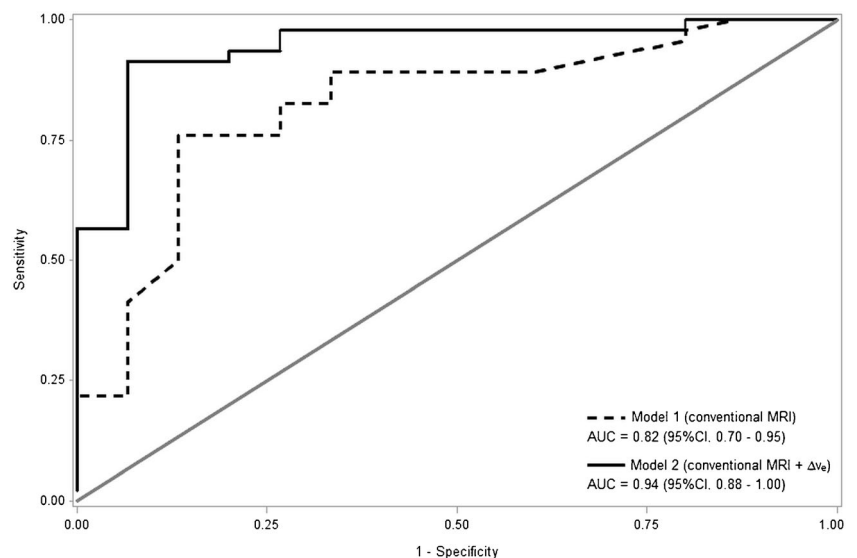
treatment subgroup (radiosurgery vs whole-brain radiotherapy vs systemic therapy). The heterogeneity of treatment strategies is inherent to the progress of histopathological and genetic characterization of lung cancer which allows for individual treatment decision [5]. Nevertheless, the strong correlation between Δv_e and the volumetric variation at midterm follow-up in each treatment subgroup supported the prognostic value of Δv_e whatever the type of treatment. Second, we only included patients with brain metastases from lung cancer whereas previous studies included various primary tumours [16, 17]. This may explain in part the moderate association between ΔK^{trans} and the objective response in this study, similarly to breast cancers in which the diagnostic accuracy of K^{trans} in predicting complete response after neoadjuvant chemotherapy depends on immunochemistry subtypes [38]. The absence of

association between survival and DCE MRI parameters may be explained by the high rate of extracranial causes of death in our study (75%), in line with others [39]. Finally, the low overall survival rate (54.5%) limited the follow-up efficiency. Surviving patients may have less active brain metastases causing a selection bias.

Conclusions

Our preliminary study showed the potential value of DCE MRI, and particularly the pharmacokinetic parameter v_e , as a biomarker of the response of brain metastases from lung cancer to anti-neoplastic therapy. The early variation of v_e may help the clinician to identify patients with high risk of progression, to

Fig. 6 ROC curves analysis for conventional MRI with and without the addition of Δv_e . The addition of Δv_e to conventional MRI in the prediction model significantly improved the diagnostic accuracy: *AUC* = 0.82 [95% CI = 0.70, 0.95] for model 1 (conventional MRI) vs *AUC* = 0.94 [95% CI = 0.88, 1.00] for model 2 (conventional MRI + Δv_e), $p = 0.03$. *AUC* area under the receiver operating characteristics curve



individualize patient's oncological follow-up and anticipate second-line treatments. Further studies including larger groups of patients are required to confirm the exact role of DCE MRI in the management of patients with brain metastases.

Compliance with ethical standards

Guarantor The scientific guarantor of this publication is Prof. Xavier Leclerc.

Conflict of interest The authors of this manuscript declare no relationships with any companies whose products or services may be related to the subject matter of the article.

Funding The authors state that this work has not received any funding.

Statistics and biometry One of the authors (Elodie Drumez) has significant statistical expertise.

Ethical approval Institutional review board approval was obtained.

Informed consent Written informed consent was obtained from all subjects (patients) in this study.

Methodology

- prospective
- diagnostic or prognostic study
- performed at one institution

References

1. Ferlay J, Steliarova-Foucher E, Lortet-Tieulent J et al (2013) Cancer incidence and mortality patterns in Europe: estimates for 40 countries in 2012. *Eur J Cancer* 49:1374–1403
2. Goncalves PH, Peterson SL, Vignea FD et al (2016) Risk of brain metastases in patients with nonmetastatic lung cancer: analysis of the Metropolitan Detroit Surveillance, Epidemiology, and End Results (SEER) data. *Cancer* 122:1921–1927
3. Peters S, Bexelius C, Munk V, Leigh N (2016) The impact of brain metastasis on quality of life, resource utilization and survival in patients with non-small-cell lung cancer. *Cancer Treat Rev* 45:139–162
4. Soffietti R, Cornu P, Delattre JY et al (2006) EFNS Guidelines on diagnosis and treatment of brain metastases: report of an EFNS Task Force. *Eur J Neurol* 13:674–681
5. Novello S, Barlesi F, Califano R et al (2016) Metastatic non-small-cell lung cancer: ESMO Clinical Practice Guidelines for diagnosis, treatment and follow-up. *Ann Oncol* 27:v1–v27
6. Lin NU, Lee EQ, Aoyama H et al (2015) Response assessment criteria for brain metastases: proposal from the RANO group. *Lancet Oncol* 16:e270–e278
7. Jakubovic R, Zhou S, Heyn C et al (2016) The predictive capacity of apparent diffusion coefficient (ADC) in response assessment of brain metastases following radiation. *Clin Exp Metastasis* 33:277–284
8. Essig M, Waschki M, Wenz F, Debus J, Hentrich HR, Knopp MV (2003) Assessment of brain metastases with dynamic susceptibility-weighted contrast-enhanced MR imaging: initial results. *Radiology* 228:193–199
9. Chernov MF, Hayashi M, Izawa M et al (2009) Dynamics of metabolic changes in intracranial metastases and distant normal-appearing brain tissue after stereotactic radiosurgery: a serial proton magnetic resonance spectroscopy study. *Neuroradiol J* 22:58–71
10. Jain R (2013) Measurements of tumor vascular leakiness using DCE in brain tumors: clinical applications. *NMR Biomed* 26:1042–1049
11. Tofts PS, Brix G, Buckley DL et al (1999) Estimating kinetic parameters from dynamic contrast-enhanced T(1)-weighted MRI of a diffusible tracer: standardized quantities and symbols. *J Magn Reson Imaging* 10:223–232
12. Piludu F, Marzi S, Pace A et al (2015) Early biomarkers from dynamic contrast-enhanced magnetic resonance imaging to predict the response to antiangiogenic therapy in high-grade gliomas. *Neuroradiology* 57:1269–1280
13. Yun TJ, Park CK, Kim TM et al (2015) Glioblastoma treated with concurrent radiation therapy and temozolomide chemotherapy: differentiation of true progression from pseudoprogression with quantitative dynamic contrast-enhanced MR imaging. *Radiology* 274:830–840
14. Tudorica A, Oh KY, Chui SY et al (2016) Early prediction and evaluation of breast cancer response to neoadjuvant chemotherapy using quantitative DCE-MRI. *Transl Oncol* 9:8–17
15. Fusco R, Sansone M, Petrillo M et al (2016) Multiparametric MRI for prostate cancer detection: preliminary results on quantitative analysis of dynamic contrast enhanced imaging, diffusion-weighted imaging and spectroscopy imaging. *Magn Reson Imaging* 34:839–845
16. Jakubovic R, Sahgal A, Soliman H et al (2014) Magnetic resonance imaging-based tumour perfusion parameters are biomarkers predicting response after radiation to brain metastases. *Clin Oncol (R Coll Radiol)* 6555:00264–00267
17. Almeida-Freitas DB, Pinho MC, Otaduy MC, Braga HF, Meira-Freitas D, da Costa Leite C (2014) Assessment of irradiated brain metastases using dynamic contrast-enhanced magnetic resonance imaging. *Neuroradiology* 56:437–443
18. Lin NU, Lee EQ, Aoyama H et al (2013) Challenges relating to solid tumour brain metastases in clinical trials, part 1: patient population, response, and progression. A report from the RANO group. *Lancet Oncol* 14:e396–e406
19. Fleiss JL (1986) Reliability of measurement. In: *The design and analysis of clinical experiments*. Wiley, Hoboken, pp 1–32
20. Sperduto PW, Kased N, Roberge D et al (2012) Summary report on the graded prognostic assessment: an accurate and facile diagnosis-specific tool to estimate survival for patients with brain metastases. *J Clin Oncol* 30:419–425
21. Schoenfeld D (1982) Partial residuals for the proportional hazards regression model. *Biometrika* 69:239–241
22. Nduom EK, Yang C, Merrill MJ, Zhuang Z, Lonser RR (2013) Characterization of the blood-brain barrier of metastatic and primary malignant neoplasms. *J Neurosurg* 119:427–433
23. Ludemann L, Grieger WN, Wurm R, Wust P, Zimmer C (2005) Quantitative measurement of leakage volume and permeability in gliomas, meningiomas and brain metastases with dynamic contrast-enhanced MRI. *Magn Reson Imaging* 23:833–841
24. Mills SJ, Soh C, Rose CJ et al (2010) Candidate biomarkers of extravascular extracellular space: a direct comparison of apparent diffusion coefficient and dynamic contrast-enhanced MR imaging-derived measurement of the volume of the extravascular extracellular space in glioblastoma multiforme. *AJNR Am J Neuroradiol* 31:549–553
25. Yankeelov TE, Lepage M, Chakravarthy A et al (2007) Integration of quantitative DCE-MRI and ADC mapping to monitor treatment response in human breast cancer: initial results. *Magn Reson Imaging* 25:1–13

26. Batchelor TT, Sorensen AG, di Tomaso E et al (2007) AZD2171, a pan-VEGF receptor tyrosine kinase inhibitor, normalizes tumor vasculature and alleviates edema in glioblastoma patients. *Cancer Cell* 11:83–95
27. Farrar CT, Kamoun WS, Ley CD et al (2011) Sensitivity of MRI tumor biomarkers to VEGFR inhibitor therapy in an orthotopic mouse glioma model. *PLoS One* 6:e17228
28. Chung C, Jalali S, Foltz W et al (2013) Imaging biomarker dynamics in an intracranial murine glioma study of radiation and antiangiogenic therapy. *Int J Radiat Oncol Biol Phys* 85:805–812
29. Kamoun WS, Ley CD, Farrar CT et al (2009) Edema control by cediranib, a vascular endothelial growth factor receptor-targeted kinase inhibitor, prolongs survival despite persistent brain tumor growth in mice. *J Clin Oncol* 27:2542–2552
30. Fortin D (2012) The blood-brain barrier: its influence in the treatment of brain tumors metastases. *Curr Cancer Drug Targets* 12: 247–259
31. Deeken JF, Loscher W (2007) The blood-brain barrier and cancer: transporters, treatment, and Trojan horses. *Clin Cancer Res* 13: 1663–1674
32. Connell JJ, Chatain G, Cornelissen B et al (2013) Selective permeabilization of the blood-brain barrier at sites of metastasis. *J Natl Cancer Inst* 105:1634–1643
33. Park EJ, Zhang YZ, Vykhodtseva N, McDannold N (2012) Ultrasound-mediated blood-brain/blood-tumor barrier disruption improves outcomes with trastuzumab in a breast cancer brain metastasis model. *J Control Release* 3659:00693–00691
34. Thorsen F, Fite B, Mahakian LM et al (2013) Multimodal imaging enables early detection and characterization of changes in tumor permeability of brain metastases. *J Control Release* 172:812–822
35. Lockman PR, Mittapalli RK, Taskar KS et al (2010) Heterogeneous blood-tumor barrier permeability determines drug efficacy in experimental brain metastases of breast cancer. *Clin Cancer Res* 16: 5664–5678
36. Patel TR, McHugh BJ, Bi WL, Minja FJ, Knisely JP, Chiang VL (2011) A comprehensive review of MR imaging changes following radiosurgery to 500 brain metastases. *AJNR Am J Neuroradiol* 32: 1885–1892
37. Cohen JV, Alomari AK, Vortmeyer AO et al (2016) Melanoma brain metastasis pseudoprogression after pembrolizumab treatment. *Cancer Immunol Res* 4:179–182
38. Drisis S, Metens T, Ignatiadis M, Stathopoulos K, Chao SL, Lemort M (2016) Quantitative DCE-MRI for prediction of pathological complete response following neoadjuvant treatment for locally advanced breast cancer: the impact of breast cancer subtypes on the diagnostic accuracy. *Eur Radiol* 26:1474–1484
39. Andrews DW, Scott CB, Sperduto PW et al (2004) Whole brain radiation therapy with or without stereotactic radiosurgery boost for patients with one to three brain metastases: phase III results of the RTOG 9508 randomised trial. *Lancet* 363:1665–1672